

# New Evidence in an Old Case: The Question of Chromium Hexafluoride Reinvestigated

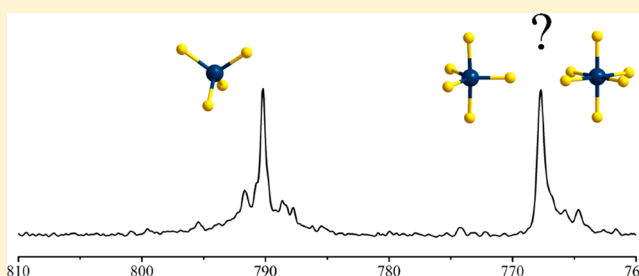
Tobias Schlöder,<sup>†</sup> Felix Brosi,<sup>†</sup> Benjamin J. Freyh,<sup>‡</sup> Thomas Vent-Schmidt,<sup>‡</sup> and Sebastian Riedel<sup>\*,†</sup>

<sup>†</sup>Institut für Chemie und Biochemie – Anorganische Chemie, Freie Universität Berlin, Fabeckstraße 34–36, D-14195 Berlin, Germany

<sup>‡</sup>Institut für Anorganische und Analytische Chemie, Albert-Ludwigs-Universität Freiburg, Albertstraße 21, D-79104 Freiburg i. Br., Germany

## Supporting Information

**ABSTRACT:** The question of whether or not the chromium hexafluoride molecule has been synthesized and characterized has been widely discussed in the literature and cannot, in spite of many efforts, yet be answered beyond doubt. New matrix-isolation experiments can now show, together with state-of-the-art quantum-chemical calculations, that the compound previously isolated in inert gas matrixes, was  $\text{CrF}_5$  and not  $\text{CrF}_6$ . New bands in the matrix IR spectra can be assigned to the  $\text{Cr}_2\text{F}_{10}$  dimer, and furthermore evidence was found in the spectra for a photodissociation or reversible excitation of  $\text{CrF}_5$  under UV irradiation. However, even if  $\text{CrF}_6$  is not stable at ambient conditions, its formation under high fluorine pressures in autoclave reactions cannot be excluded completely.



## INTRODUCTION

Is chromium hexafluoride a stable compound? Almost 50 years after the first report of its synthesis by Roesky and Glemser in 1963<sup>1</sup> this question could not yet be unambiguously answered. The VI oxidation state of chromium is however well known,<sup>2</sup> as in the anionic oxochromates(VI)  $[\text{CrO}_4]^{2-}$  and  $[\text{Cr}_2\text{O}_7]^{2-}$  as well as in their anhydrous form, chromium trioxide. Further, the oxide fluorides  $\text{CrO}_2\text{F}_2$  and  $\text{CrOF}_4$  are stable molecules and were studied in the solid state<sup>3–5</sup> as well as in the gas phase.<sup>6,7</sup> Yet, the highest neutral binary fluoride of chromium characterized beyond doubt is  $\text{CrF}_5$ , a deep red solid with a melting point of 30 °C.<sup>4,8</sup> Furthermore, the  $[\text{CrF}_5]^+$  cation with chromium in its formal oxidation state VI was observed in mass spectrometric experiments.<sup>9</sup> However, it is unclear whether it was formed by ionization of neutral chromium pentafluoride or by fluoride abstraction from chromium hexafluoride.

The parent compound,  $\text{CrF}_6$ , was claimed to be synthesized after high-pressure fluorination of either elemental chromium or  $\text{CrO}_3$ . The first synthesis starting from chromium powder was conducted at 400 °C, and a fluorine pressure of 350 atm was used. A lemon yellow product together with deep red chromium pentafluoride was observed. On the basis of elemental analysis the yellow product was identified to be  $\text{CrF}_6$ .<sup>1</sup> In the second synthesis, the use of chromium trioxide as the starting material was described. The use of  $\text{CrO}_3$  allowed somewhat milder reaction conditions (170 °C, 25 atm), which also led to the formation of both yellow  $\text{CrF}_6$  and red  $\text{CrF}_5$ .<sup>10,11</sup>

Both chromium hexafluoride and chromium pentafluoride were subsequently evaporated and isolated in inert gas matrixes. The recorded infrared spectra showed strong absorptions at

767.7  $\text{cm}^{-1}$  (neon matrixes), 763.2  $\text{cm}^{-1}$  (argon matrixes), and 758.9  $\text{cm}^{-1}$  ( $\text{N}_2$  matrixes), which all exhibited the typical isotopic pattern due to the different chromium isotopes in their natural abundances. In addition, the absorptions due to  $\text{CrF}_4$  were also observed in the spectra and were much stronger when  $\text{CrF}_5$  was evaporated. Odgen et al. concluded from these observations that the new band is caused by the octahedral  $\text{CrF}_6$  molecule, whose expectation IR spectrum contains only one single IR-active mode in the region of the Cr–F stretching vibrations, and that  $\text{CrF}_5$  disproportionates upon evaporation.<sup>10–12</sup> Later, the experiments were repeated by Willner et al., who offered a different explanation for the observed spectra, which were very similar to those obtained before.<sup>13,14</sup> They concluded that the new band should be assigned to  $\text{CrF}_5$  instead of  $\text{CrF}_6$ . This was based on their observation that gaseous  $\text{CrF}_5$  showed no tendency to disproportionate and did not decompose when being expanded into the vacuum. However, the expectation spectrum of the  $C_{2v}$ -symmetrical chromium pentafluoride molecule consists of several IR-active Cr–F stretching fundamentals. Willner et al. therefore suggested that the intensities of the three  $A_1$  modes would be too low to be observed and that the two remaining bands (corresponding to the  $B_1$  and  $B_2$  modes) would have almost the same wavenumber.<sup>13</sup> In their more detailed second investigation of chromium fluorides, a second broad band could be assigned to  $\text{CrF}_5$ , which overlaps with the bands of  $\text{CrF}_4$  and which might have been overlooked in the previous study.<sup>14</sup>

Received: March 24, 2014

Published: May 15, 2014

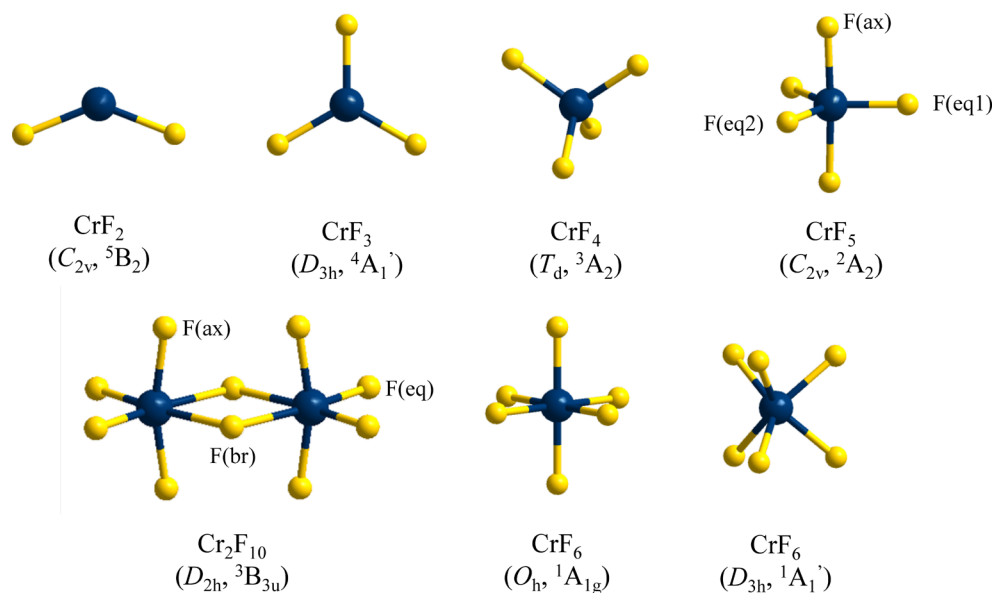


**Figure 1.** Optimized structures of molecular chromium fluorides; see Table 1 for bond lengths and angles.

Besides these experimental studies, the chromium hexafluoride molecule was also investigated by quantum-chemical methods. However, the main question addressed in these studies was the structure of  $\text{CrF}_6$  and unfortunately not its stability. Despite the initial proposition of a trigonal prismatic structure ( $D_{3h}$  symmetry),<sup>15</sup> there is no doubt today that, if it exists,  $\text{CrF}_6$  would be octahedral.<sup>16–19</sup> The thermochemistry of the higher chromium fluorides was investigated only by DFT calculations, which indicate  $\text{CrF}_6$  to be stable against the loss of one fluorine atom.<sup>19</sup> Very recently, a new DFT investigation of chromium fluoride molecules was published by Siddiqui in which the elimination of a fluorine atom or molecule from  $\text{CrF}_6$  was predicted to be endothermic.<sup>20</sup> However, no values were given for the enthalpies of dissociation, and the findings presented in this study are unlikely to be reliable in general, as a triplet (!) ground state was predicted for chromium hexafluoride, which is impossible for the  $d^0$  electron configuration of  $\text{Cr}^{\text{VI}}$  and furthermore in disagreement with all previous investigations of this molecule. In addition, it is well known that DFT calculations can fail in the prediction of thermochemical values due to significant nondynamical correlation effects; see ref 21.

We therefore reinvestigated this long-standing question by new matrix-isolation experiments, using on the one hand the laser-ablation technique to generate excited Cr atoms, which were then reacted with  $\text{F}_2$ , and, on the other hand,  $\text{CrF}_5$  presynthesized by autoclave techniques, which was then evaporated and condensed at the cold window under an excess of argon, neon, or neat fluorine. We furthermore predicted thermochemical stabilities and vibrational spectra of high-valent chromium fluorides using state-of-the-art quantum-chemical methods up to the CCSD(T) level. Most of the quantum-chemical studies as well as the laser-ablation experiments presented in this article were done as part of the doctoral thesis of coauthor T.S.<sup>22</sup> The corresponding reference is given at the beginning of the respective sections. The introduction to this article is to a large part also taken from the introduction to the corresponding section 5.1 of his thesis.

## EXPERIMENTAL AND THEORETICAL METHODS

**Caution:** Fluorine and chromium fluorides are powerful oxidizers and toxic. Suitable shielding and protective clothing and face masks are necessary. Extensive care must be taken to avoid contact between the fluorides and oxidizable materials.

**High-Pressure Synthesis.** Bulk  $\text{CrF}_5$  was synthesized according to the method published by Christie.<sup>23</sup> In the glovebox,  $\text{CrF}_3$  (kindly provided by Dr. F. Kraus, powder X-ray pure) was loaded into a passivated stainless steel reactor (150 cm<sup>3</sup>), after which  $\text{F}_2$  (99.8%, Solvay Fluor GmbH) was added at  $-196$  °C. The vessel was then heated to 265 °C for 68 h, after which the remaining  $\text{F}_2$  was pumped off at  $-196$  °C. After heating to room temperature, the reaction products were condensed to prefluorinated PTFE tubes for analysis, and  $\text{CrF}_5$  was identified by its Raman spectrum.

**Matrix Isolation Experiments.** Matrix samples of in situ generated chromium fluorides were prepared by co-deposition of laser-ablated excited chromium atoms (99.9%, Smart Elements) with  $\text{F}_2$  (99.8%, Solvay Fluor GmbH) diluted at different concentrations in neon (99.999%, Air Liquide) or argon (99.999%, Sauerstoffwerk Friedrichshafen) as well as neat fluorine. The gases were mixed in a custom-made stainless steel mixing chamber equipped with a manometer, to which the neon and argon bottles as well as a stainless steel  $\text{F}_2$  storage cylinder were connected. During the preparation of the gas mixtures the fluorine cylinder was cooled to 77 K in order to freeze out possible impurities. However, some impurities such as HF,  $\text{COF}_2$ , or  $\text{SiF}_4$  have been observed in the spectra in significant amounts. The mixing vessel was connected to the matrix chamber by a stainless steel capillary. Reactants were condensed onto KBr and CsI windows cooled to 3.8–5.0 K (neon) or 10.0 K (argon and  $\text{F}_2$ ) using a closed-cycle helium cryostat (Sumitomo Heavy Industries, RDK-205D) inside the vacuum chamber. The cold windows were coated with a protective argon layer before condensing neat fluorine matrices. For the laser ablation of chromium, the 1064 nm fundamental of a Nd:YAG laser (Continuum, Minilite II; repetition rate 10 Hz, pulse width 5 ns) was focused onto a rotating chromium target through a hole in the cold window. The pulse energy of the laser was adjusted to the metal, and the best spectra were obtained using laser energies of 32 mJ per pulse. Irradiation of the matrix samples was done using a mercury arc street lamp (Osram HQL 250) with the outer globe removed and different high-pass filters (Schott; types N-WG280, N-WG320, GG400, OG515, and RG630). Matrix samples of presynthesized chromium pentafluoride were generated by co-deposition of  $\text{CrF}_5$  with argon or neon. The reaction vessel for the  $\text{CrF}_5$  synthesis was directly connected to the spray-on line system of

Table 1. Calculated and Experimental Structural Parameters of Molecular Chromium Fluorides<sup>a</sup>

molecule	parameter <sup>b</sup>	B3LYP <sup>c</sup>	CCSD(T) <sup>c</sup>	expt <sup>d</sup>	ref
CrF <sub>2</sub> (C <sub>2v</sub> , <sup>5</sup> B <sub>2</sub> )	<i>d</i> <sub>Cr-F</sub>	178.0	179.8	179.2(5)	36
		136.7	143.8		
CrF <sub>3</sub> (D <sub>3h</sub> , <sup>4</sup> A <sub>2</sub> )	<i>d</i> <sub>Cr-F</sub>	173.7	173.7	173.2(2)	39
CrF <sub>4</sub> (Td, <sup>3</sup> A <sub>2</sub> )	<i>d</i> <sub>Cr-F</sub>	171.4	170.9	170.6(2)	38
CrF <sub>5</sub> (C <sub>2v</sub> , <sup>2</sup> A <sub>2</sub> )	<i>d</i> <sub>Cr-F(ax)</sub>	174.7	173.8	174.2(10)	37
	<i>d</i> <sub>Cr-F(eq1)</sub>	168.2	167.3	169.5(6) <sup>e</sup>	
	<i>d</i> <sub>Cr-F(eq2)</sub>	169.8	170.1		
	<F(eq1)-Cr-F(ax)	91.4	94.2		
	<F(eq1)-Cr-F(eq2)	121.8	119.7		
	<F(eq1)-Cr-F(eq2)	172.9	172.4		
CrF <sub>6</sub> (O <sub>h</sub> , <sup>1</sup> A <sub>1g</sub> )	<i>d</i> <sub>Cr-F</sub>	172.9	172.4		
CrF <sub>6</sub> (D <sub>3h</sub> , <sup>1</sup> A <sub>1</sub> )	<i>d</i> <sub>Cr-F</sub>	173.9	173.4		
		<F-Cr-X <sup>f</sup>	50.4	50.4	
Cr <sub>2</sub> F <sub>10</sub> (D <sub>2h</sub> , <sup>3</sup> B <sub>3u</sub> )	<i>d</i> <sub>Cr-F(ax)</sub>	170.0			
	<i>d</i> <sub>Cr-F(eq)</sub>	171.0			
	<i>d</i> <sub>Cr-F(br)</sub>	198.2			
	<F(br)-Cr-F(br)	76.5			
	<F(br)-Cr-F(eq)	94.1			
	<F(br)-Cr-F(ax)	84.1			

<sup>a</sup>Bond lengths in pm, angles in deg. <sup>b</sup>See Figure 1 for atom labeling. <sup>c</sup>aVTZ basis sets. <sup>d</sup>*r*<sub>g</sub> values from GED measurements; nozzle temperatures 1520 K for CrF<sub>2</sub>, 1220 K for CrF<sub>3</sub>, 195–220 °C for CrF<sub>4</sub>, and 80 °C for CrF<sub>5</sub>. <sup>e</sup>Measured averaged bond length *d*<sub>Cr-F(eq)</sub>. <sup>f</sup>Angle between the Cr–F bond and the C<sub>3</sub> axis.

the matrix chamber, and the vapor pressure at room temperature was used for deposition. Infrared spectra were recorded on a Bruker Vertex 70 FT-IR spectrometer purged with dry air at 0.5 cm<sup>-1</sup> resolution in the region between 4000 and 450 cm<sup>-1</sup> using an RT-DLaTGS or liquid-nitrogen-cooled MCT-B detector.

**Quantum-Chemical Calculations.** The structures of all molecules were fully optimized (by relaxing all parameters) at density functional theory level using the B3LYP<sup>24–27</sup> hybrid functional, which was shown to provide reliable results for comparable molecules.<sup>28,29</sup> Dunning's correlation-consistent triple- $\xi$  aug-cc-pVTZ (denoted as aVTZ for brevity) basis sets were used for both fluorine and chromium.<sup>30,31</sup> Relativistic effects were not considered in the calculations, as they are of minor importance for these light elements. The ground states of all molecules were determined by calculating the structures of all possible allowed spin multiplicities arising from the respective *d*<sup>n</sup> electron configurations of chromium. Highly symmetrical stationary points on the potential energy surface were computed within the restrictions of the respective point groups, especially when not corresponding to the (global) minimum structures. The subsequent ab initio structure optimizations at the CCSD(T) level were done starting from the structures optimized at the DFT level while retaining the molecular symmetries. The ROHF reference function has been used in the case of open-shell electron configurations. In ab initio calculations the frozen core approximation was used for the 1s orbitals of fluorine as well as the 1s, 2sp, and 3sp orbitals of chromium.

Harmonic frequency calculations were carried out for the stationary points on the potential energy surface for different possible isotopomers. The extrapolation of the thermochemical values to the complete basis set (CBS) limit<sup>32</sup> was done using different correlation-consistent basis sets (aug-cc-pVXZ, X = D, T, Q).<sup>30,31</sup> Whereas the Hartree–Fock energy was extrapolated by an exponential fit ( $E_{\text{HF}}(X) = E_{\text{HF}}(\text{CBS}) + B e^{-cX}$ ), the correlation energy at the CBS limit was obtained using an expression of the form  $E_{\text{corr}}(X) = E_{\text{corr}}(\text{CBS}) + BX^{-3}$ . The influence of core–valence correlation on the thermochemical values at the CCSD(T) level was evaluated by single-point calculations using the aug-cc-pwCVTZ-NR basis sets (denoted as awCVTZ-NR)<sup>31,33</sup> and corresponding smaller frozen cores (F: none, Cr: 1s2sp). For each molecule, two CCSD(T)/awCVTZ//CCSD(T)/aVTZ calculations were done with both the small (sFC) and the large frozen core (lFC), and the difference  $\Delta E_{\text{CV}} = E_{\text{sFC}} - E_{\text{lFC}}$  was used as an additive correction. The calculations at the DFT and ab initio level

were done using the Gaussian09<sup>24</sup> and CFOUR<sup>34</sup> program packages, respectively.

## RESULTS AND DISCUSSION

**Calculated Structures, Thermochemistry, and Vibrational Frequencies (ref 22).** The structures of the binary chromium fluoride molecules were optimized at the CCSD(T) level and are shown in Figure 1. All molecules were found to have high-spin ground states with a maximum number of unpaired electrons (Table 1). For CrF<sub>2</sub>, a C<sub>2v</sub>-symmetrical bent structure (*d*<sub>Cr-F</sub> = 179.8 pm,  $\angle_{\text{F-Cr-F}} = 143.8^\circ$ ) was calculated and agrees well with a previous computational investigation.<sup>35</sup> Both chromium trifluoride and chromium tetrafluoride have highly symmetrical structures of D<sub>3h</sub> and T<sub>d</sub> symmetry, respectively, and the bond lengths were calculated to be 173.7 pm in CrF<sub>3</sub> and 170.9 pm in CrF<sub>4</sub>. For CrF<sub>5</sub>, the single unpaired electron leads to a Jahn–Teller distorted trigonal bipyramidal structure of C<sub>2v</sub> symmetry. The vibronically unstable <sup>2</sup>E' state of the regular D<sub>3h</sub>-symmetrical structure reduces to <sup>2</sup>A<sub>2</sub> + <sup>2</sup>B<sub>1</sub> in C<sub>2v</sub> symmetry, and both states were optimized at the CCSD(T) level. The <sup>2</sup>A<sub>2</sub> state was calculated to be a minimum, marginally lower in energy (0.6 kJ mol<sup>-1</sup> at the CCSD(T)/CBS level) than the <sup>2</sup>B<sub>1</sub> state, which was found to be a transition state. Due to the 3-fold rotation axis in the D<sub>3h</sub> point group, a “mexican hat”-like potential energy surface was computed. This “mexican hat” potential shows three <sup>2</sup>A<sub>2</sub> minima, which are connected by three <sup>2</sup>B<sub>1</sub> transition states. Based on this flat potential, the molecule is most probably fluxional at already moderate temperatures. Figure 2 shows a scan of this potential energy surface, which was calculated by optimizing the structure of CrF<sub>5</sub> in D<sub>3h</sub> symmetry and subsequently displacing the chromium atom in the equatorial plane of the trigonal bipyramidal transition state. As the positions of the fluorine atoms were fixed during their calculations, only an approximate potential energy surface was obtained. Nevertheless, its trigonal symmetry as well as the three minima and transition states can be recognized. The calculated bond lengths in the <sup>2</sup>A<sub>2</sub> minimum structure are *d*<sub>F(ax)</sub>



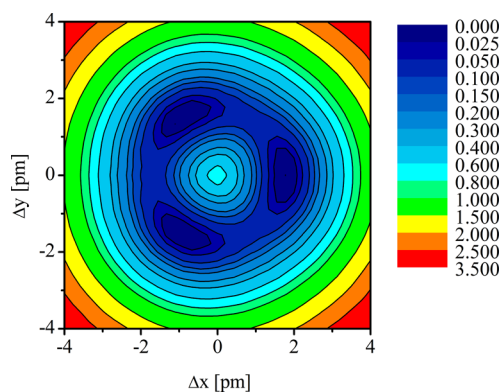


**Figure 2.** Scan of the “mexican hat” potential energy surface of  $\text{CrF}_5$  at the B3LYP/aVTZ level. The energy is plotted as a function of the displacement of the chromium atom from the center of a trigonal bipyramidal structure (see text); values in  $\text{kJ mol}^{-1}$ .

= 173.8 pm,  $d_{\text{F}(\text{eq}1)} = 167.3$  pm, and  $d_{\text{F}(\text{eq}2)} = 170.1$  pm. Finally, an octahedral structure ( $O_h$  symmetry) with a chromium–fluorine distance of 172.4 pm was calculated for chromium hexafluoride. The trigonal prismatic conformer of this molecule was also calculated to be  $45.6 \text{ kJ mol}^{-1}$  higher in energy at the CCSD(T)/CBS level of theory. Furthermore, this structure shows one imaginary frequency at  $95.2 \text{ cm}^{-1}$  at the CCSD(T)/aVTZ level and is therefore in line with the above-mentioned previous investigations in which the  $O_h$ -symmetrical conformer was also obtained as the minimum structure. The average Cr–F bond lengths in the lower chromium fluorides decrease with increasing oxidation state of the metal and reach a minimum for  $\text{CrF}_4$  and  $\text{CrF}_5$ , which can be explained by the higher charge at the central atom, which leads to more polarized and stronger bonds. By contrast, the bond length increases again for  $\text{CrF}_6$ , thus hinting at the steric crowding in the ligand sphere, prohibiting an ideal relaxation of the bond length. Beyond these mononuclear compounds, the  $\text{Cr}_2\text{F}_{10}$  dimer has also been computed at the B3LYP/aVTZ level. It shows a  $D_{2h}$ -symmetrical structure consisting of two edge-sharing  $\text{CrF}_4\text{F}_{2/2}$  octahedra. The calculated ground state of this molecule is  $^3\text{B}_{3w}$  and the terminal Cr–F bond lengths of  $d_{\text{F}(\text{eq})} = 171.0$  pm and  $d_{\text{F}(\text{ax})} = 170.0$  pm are similar to those of the monomer, whereas expectedly the Cr–F distances are significantly larger for the bridging fluorine atoms (198.2 pm).

For all monomeric chromium fluorides except the elusive  $\text{CrF}_6$ , experimental gas phase structures were obtained by electron diffraction measurements.<sup>36–39</sup> With the exception of  $\text{CrF}_5$ , the calculated bond lengths were slightly smaller than the experimental ones (Table 1). These differences between the experimental and the computed values would increase if the effects of the elevated temperatures of the experiments were considered, especially for the lower fluorides, for the evaporation of which higher temperatures were necessary. The agreement between the calculated and measured bond lengths thus significantly increases with increasing oxidation state of the metal, which can be explained by the reduced importance of core–valence correlation in the higher-valent fluorides: It was shown before that the consideration of core–valence correlation in the structure optimizations leads to a shortening of the bonds in comparable molecules,<sup>40</sup> which is more pronounced for lower oxidation states of the metal.<sup>28</sup>

To answer the question of the thermochemical stability of chromium hexafluoride, three different possible decomposition

reactions were calculated (Table 2). At the DFT level only the bimolecular  $\text{F}_2$  elimination is found to be exothermic, whereas

**Table 2.** Calculated Thermochemistry of  $\text{CrF}_6$  and  $\text{CrF}_5$ <sup>a</sup>

reaction	B3LYP <sup>b</sup>		CCSD(T) <sup>c</sup>	
$\text{CrF}_6 \rightarrow \text{CrF}_4 + \text{F}_2$	23.6	(14.5)	−22.3	(−32.3)
$\text{CrF}_6 \rightarrow \text{CrF}_5 + \text{F}$	55.3	(47.7)	30.3	(23.2)
$\text{CrF}_6 \rightarrow \text{CrF}_5 + 1/2 \text{F}_2$	−22.4	(−26.8)	−46.1	(−50.4)
$\text{CrF}_5 \rightarrow \text{CrF}_3 + \text{F}_2$	339.7	(329.6)	303.1	(294.6)
$\text{CrF}_5 \rightarrow \text{CrF}_4 + \text{F}$	123.6	(115.8)	100.4	(91.7)
$\text{CrF}_5 \rightarrow \text{CrF}_4 + 1/2 \text{F}_2$	46.0	(41.3)	24.1	(18.1)
$\text{CrF}_5 \rightarrow 1/2 \text{CrF}_6 + 1/2 \text{CrF}_4$	34.2	(34.0)	52.2	(55.5)
$\text{CrF}_5 \rightarrow 1/2 \text{Cr}_2\text{F}_{10}$	−11.7	(−8.6)		

<sup>a</sup>Energies in  $\text{kJ mol}^{-1}$ ; values in parentheses are ZPE corrected. <sup>b</sup>aVTZ basis sets. <sup>c</sup>Extrapolated to the CBS limit and corrected for CV effects, ZPE correction using the aVTZ basis sets.

the unimolecular elimination of difluorine (yielding  $\text{CrF}_4$ ) is thermochemically favored at the CCSD(T) level as well. For comparison, the same decomposition reactions were all calculated to be endothermic for the experimentally verified  $\text{CrF}_5$  molecule. The claimed synthesis of chromium hexafluoride was conducted at high temperatures and high fluorine pressures. According to the principle of Le Châtelier, these conditions favor the formation of  $\text{CrF}_6$ . Furthermore, there are in principle good arguments for a kinetic stability of this molecule. First, the unimolecular  $\text{F}_2$  elimination leading to  $\text{CrF}_4$  is spin-forbidden, as this latter molecule has a triplet ground state. The lowest-lying singlet state of  $\text{CrF}_4$  was computed to be  $156.1 \text{ kJ mol}^{-1}$  above the triplet ground state at the CCSD(T)/CBS level. The corresponding spin-allowed  $\text{F}_2$  elimination reaction would therefore be endothermic. Second, the bimolecular elimination of  $\text{F}_2$  probably has a high activation barrier due to the negatively charged ligand spheres of the two  $\text{CrF}_6$  molecules. If matrix-isolated molecules are considered, this reaction is most likely inhibited by the solid inert environment.

It can therefore not be completely excluded that  $\text{CrF}_6$  was actually synthesized and survived the transfer to the inert matrixes as a metastable species. As the experimental matrix IR spectra of the vapor phases above samples of  $\text{CrF}_5$  and the supposed  $\text{CrF}_6$  were identical, it was suggested that  $\text{CrF}_5$  disproportionates to yield  $\text{CrF}_4$  and  $\text{CrF}_6$ . This disproportionation was therefore also quantum chemically investigated, showing that the energy of reaction is endothermic by  $+56.4 \text{ kJ mol}^{-1}$  at the coupled-cluster level, indicating that the reaction is unlikely to proceed and therefore confirming the experimental observation that gaseous  $\text{CrF}_5$  is stable against disproportionation. However, lattice effects were not considered in the calculation, and the difference between the lattice enthalpies of  $\text{CrF}_4$  and  $\text{CrF}_5$  might actually lead to an overall exothermicity of the disproportionation reaction due to the additional stabilization of solid  $\text{CrF}_4$  as the product. Furthermore, the dimerization of  $\text{CrF}_5$  was also calculated, and the formation of  $\text{Cr}_2\text{F}_{10}$  was found to be exothermic by  $8.6 \text{ kJ mol}^{-1}$  at the B3LYP/aVTZ level.

The vibrational spectra of the matrix-isolated lower chromium fluorides  $\text{CrF}_2$ ,  $\text{CrF}_3$ , and  $\text{CrF}_4$  are experimentally well known, and there is no doubt about the assignment of their bands.<sup>11,14,41,42</sup> All these compounds show the expected splitting due to the different isotopes of chromium in their natural abundances (<sup>50</sup>Cr: 4.3%, <sup>52</sup>Cr: 83.8%, <sup>53</sup>Cr: 9.5%, and

Table 3. Calculated and Observed Wavenumbers of Molecular Chromium Fluorides<sup>a</sup> in the 400–100 cm<sup>-1</sup> Region

molecule	mode	calcd				expt (matrix)	
		B3LYP <sup>b</sup>		CCSD(T) <sup>b</sup>		Ne	Ar
CrF <sub>2</sub> (C <sub>2v</sub> , <sup>5</sup> B <sub>2</sub> )	A <sub>1</sub>	617.8	(56)				
	B <sub>2</sub>	721.4	(235)			679.5	654.4
CrF <sub>3</sub> (D <sub>3h</sub> , <sup>4</sup> A <sub>2</sub> ')	A <sub>1</sub> '	669.5	(–)	678.8	(–)		
	E'	759.0	(469)	761.9	(537)	762.8 <sup>c</sup>	749.3
CrF <sub>4</sub> (T <sub>d</sub> , <sup>3</sup> A <sub>2</sub> )	A <sub>1</sub>	713.9	(–)	722.1	(–)		
	T <sub>2</sub>	783.5	(602)	799.7	(669)	790.2 <sup>c</sup>	784.3 <sup>d</sup>
CrF <sub>5</sub> (C <sub>2v</sub> , <sup>2</sup> A <sub>2</sub> )	A <sub>1</sub>	608.9	(0)	623.9	(0)		
	A <sub>1</sub>	720.6	(0)	720.1	(0)		
	B <sub>1</sub>	727.7	(310)	790.1	(337)	767.7 <sup>c</sup>	763.1 <sup>d</sup>
	B <sub>2</sub>	763.5	(324)	809.5	(222)	791.5	785.9
CrF <sub>6</sub> (O <sub>h</sub> , <sup>1</sup> A <sub>1g</sub> )	A <sub>1</sub>	828.3	(209)	844.2	(211)		
	E <sub>g</sub>	587.2	(–)	589.9	(–)		
	A <sub>1g</sub>	708.2	(–)	716.8	(–)		
Cr <sub>2</sub> F <sub>10</sub> (D <sub>2h</sub> , <sup>3</sup> B <sub>3u</sub> )	T <sub>1u</sub>	761.0	(939)	785.3	(1019)		
	B <sub>3u</sub>	407.6	(268)			415.8	414.3
	B <sub>1u</sub>	428.5	(31)				431.6
	A <sub>g</sub>	466.8	(–)				
	B <sub>3u</sub>	690.3	(59)			672.9	672.8
	A <sub>g</sub>	691.3	(–)				
	B <sub>2g</sub>	740.8	(–)				
	B <sub>3u</sub>	745.5	(481)			735.5	731.9
	B <sub>1u</sub>	775.3	(333)			766.8	763.1
	A <sub>g</sub>	778.5	(–)				
	B <sub>1g</sub>	786.8	(–)				
B <sub>2u</sub>	831.8	(477)			816.3	812.6	

<sup>a</sup>Values in cm<sup>-1</sup> for <sup>52</sup>Cr isotopomers; numbers in parentheses are infrared intensities in km mol<sup>-1</sup>. <sup>b</sup>aVTZ basis sets. <sup>c</sup>Published values: 790.17 cm<sup>-1</sup> for CrF<sub>4</sub> and 767.71 cm<sup>-1</sup> for CrF<sub>5</sub>. <sup>d</sup>Published values: 784.3 cm<sup>-1</sup> for CrF<sub>4</sub> and 763.2 cm<sup>-1</sup> for CrF<sub>5</sub> (assigned to CrF<sub>6</sub>).<sup>11,12</sup>

<sup>54</sup>Cr: 2.4%). By contrast, the origin of the band observed at 763.0 cm<sup>-1</sup> in argon and 767.7 cm<sup>-1</sup> in neon matrixes is so far unclear.<sup>10–14</sup> This band shows the typical isotopic pattern of chromium and was observed in the matrix IR spectra obtained after the thermal evaporation of samples of either CrF<sub>5</sub> or the putative CrF<sub>6</sub>. It was subsequently attributed to both of these molecules, and the correct assignment is still under debate. In order to solve this long-standing problem, the harmonic frequencies of the chromium fluoride molecules were computed at the CCSD(T)/aVTZ level; see Table 3. The computed wavenumbers of CrF<sub>3</sub> and CrF<sub>4</sub> agree well with the experimental values. [Despite many efforts, the CCSD(T)/aVTZ frequency calculations yielded only an unreasonably high wavenumber of 928.1 cm<sup>-1</sup> for CrF<sub>2</sub>, although the structure is almost the same as that obtained in a previous study in which a value of 748 cm<sup>-1</sup> was obtained at the CCSD(T)/6-311G(d) level.<sup>35</sup>] The difference between the calculated and experimental wavenumber is only 0.9 cm<sup>-1</sup> for chromium trifluoride but 5.9 cm<sup>-1</sup> for chromium tetrafluoride. This larger deviation in the case of CrF<sub>4</sub> can be explained by the reduced importance of core–valence correlation for high oxidized metals, as it was previously shown by us in the case of the comparable iron fluoride molecules.<sup>28</sup> Despite the small deviations, these frequency calculations are nevertheless very accurate and can be expected to give reliable results for CrF<sub>5</sub> and CrF<sub>6</sub> as well.

In principle only one single IR-active Cr–F stretching fundamental is expected for the octahedral CrF<sub>6</sub> molecule. Indeed, the harmonic frequency calculations at the CCSD(T)/aVTZ level show only one mode at 785.3 cm<sup>-1</sup>. At first glance, this value agrees well with the ambiguously assigned experimental band of CrF<sub>6</sub>, especially if we keep in mind that

the consideration of anharmonic corrections would further decrease the difference between the calculated and the experimental wavenumber of 767.7 cm<sup>-1</sup> in neon matrixes. Moreover, the computed isotopic shifts are also in good agreement with the experimental findings (Table S1). In the case of CrF<sub>5</sub> all computed Cr–F stretching vibrations of the C<sub>2v</sub>-symmetrical molecule are in principle IR active. Nevertheless, only three of these modes, at 790.1, 809.5, and 844.2 cm<sup>-1</sup>, are calculated to show considerable IR intensities at the CCSD(T) level.

At this point it seems clear that, based on the first experimental attempts only where one single band was observed in the spectra, this band must logically be assigned to CrF<sub>6</sub>. However, the general observations made by Willner et al. about the stability of CrF<sub>5</sub>, which did not show any tendency to disproportionate, contradicts the hypothesis of the formation of CrF<sub>6</sub>, at least in the gas phase. This outcome is also supported by the coupled-cluster calculations (vide supra). Furthermore, in their first publication Willner et al. assigned the band in question to chromium pentafluoride, arguing that only two of its Cr–F stretching modes would show a significant IR intensity and that furthermore these two absorptions would overlap to form only one single band.<sup>13</sup> Hence, if that were the case, CrF<sub>5</sub> and CrF<sub>6</sub> would be indistinguishable by IR spectroscopy. Anyway, in a more detailed second investigation of Willner et al. another broad band that was attributed to CrF<sub>5</sub> was identified.<sup>14</sup> If the corresponding third band were even broader, it might not be observed in the spectra, thus giving an alternative explanation for the concordance of the experimental spectrum of CrF<sub>5</sub> with the expectation spectrum of CrF<sub>6</sub>. This interpretation is supported by the calculated wavenumber and

isotopic shifts for the  $B_1$  Cr–F stretching mode of  $\text{CrF}_5$ , which shows a behavior very similar to that of the  $T_{1u}$  mode of  $\text{CrF}_6$ . This  $B_1$  mode corresponds to the antisymmetric F(ax)–Cr–F(ax) stretching vibration of  $\text{CrF}_5$ , whereas the remaining two high IR intensities of the  $A_1$  and  $B_2$  modes correspond to the Cr–F stretching vibrations in the equatorial plane. One might speculate that the flat potential energy surface in the equatorial plane is responsible for the extreme broadness of the two latter bands and that the experimentally observed absorption corresponds to the  $B_1$  vibration of  $\text{CrF}_5$ .

#### Laser-Ablation Matrix-Isolation Experiments (ref 22).

Matrix-isolated chromium fluoride molecules can either be generated directly during the matrix-isolation experiment or be synthesized in bulk and then be evaporated to the matrixes. Using the former method, several ways exist for the in situ generation of chromium fluorides. In a previous study, pieces of chromium were reacted with elemental fluorine at elevated temperatures, and the highest chromium fluoride obtained this way was  $\text{CrF}_4$ .<sup>43</sup> Another approach is based on the laser-ablation technique for the generation of highly reactive excited metal atoms, which can then react with  $\text{F}_2$  to form the corresponding fluoride molecules.

In the present work, laser-ablated chromium atoms were condensed together with  $\text{F}_2$  under excess neon or argon at cryogenic temperatures of 5.0 and 10.0 K, respectively. Using a  $\text{F}_2$  concentration of 0.5% in neon, three major groups of absorptions were observed directly after deposition; see Figure 3. By comparison with published values<sup>14,42</sup> these bands could

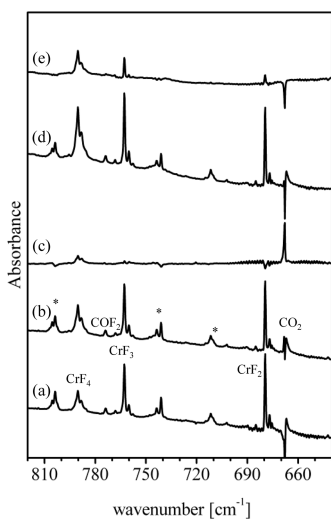


**Figure 3.** IR spectra in the 820–640  $\text{cm}^{-1}$  region obtained after co-deposition of laser-ablated chromium atoms with 0.5%  $\text{F}_2$  diluted in neon. (a) After 30 min of sample deposition at 5.0 K. (b) After annealing to 9.0 K. (c) Difference spectrum (spectrum after annealing minus spectrum directly after deposition). (d) After broadband UV irradiation with  $\lambda > 200$  nm. (e) Difference spectrum (spectrum after irradiation minus spectrum after annealing). \* denotes impurities of  $\text{F}_2$ .

be assigned to the lower fluorides  $\text{CrF}_2$ ,  $\text{CrF}_3$ , and  $\text{CrF}_4$ ; see Table 4. When the matrix samples were annealed to 9.0 K, the bands of  $\text{CrF}_4$  slightly increased at the expense of the  $\text{CrF}_2$  absorptions, and further UV irradiation of the matrixes using the full spectrum of a mercury arc lamp led to a growth of all observed chromium fluoride bands. The photochemistry of the matrix samples was investigated in more detail by irradiating the

**Table 4.** Observed Bands in the Matrix Isolation Experiments and Their Assignment

molecule	Ne	Ar	$\text{F}_2$
$^{50}\text{CrF}_2$	685.1		
$^{52}\text{CrF}_2$	679.5	654.4	
$^{53}\text{CrF}_2$	676.9		
$^{54}\text{CrF}_2$			
$^{50}\text{CrF}_3$	768.0		
$^{52}\text{CrF}_3$	762.8	749.3	
$^{53}\text{CrF}_3$	760.1	746.8	
$^{54}\text{CrF}_3$	757.7		
$^{50}\text{CrF}_4$	795.4	789.4	
$^{52}\text{CrF}_4(\text{site})$	791.7	785.6	
$^{52}\text{CrF}_4$	790.2	784.3	784.2/788.7
$^{53}\text{CrF}_4$	787.8	782.0	
$^{54}\text{CrF}_4$	785.5	779.4	
$^{50}\text{CrF}_5 (B_1)$	774.2	769.5	
$^{52}\text{CrF}_5 (B_1)$	767.7	763.1	764.2
$^{53}\text{CrF}_5 (B_1)$	764.7	760.1	761.1
$^{54}\text{CrF}_5 (B_1)$	761.6	757.1	
$\text{CrF}_5 (B_2)$	791.5	785.9	
$\text{CrF}_5^*$	790.3	788.2	787.3
	788.3	786.9	783.9
	779.0	778.3	
$\text{CrO}_2\text{F}_2$	788.6		
	726.3		
$\text{CrOF}_4$	754.9	750.9	
	750.4	746.6	
$\text{Cr}_2\text{F}_{10}$	816.3	812.6	
	766.8	763.1	
	735.5	731.9	
	672.9	672.8	
		431.6	
	415.8	414.3	

sample using different high-pass filters of successive lower wavenumber edges (Figure S2). No changes were observed in the spectra when using  $\lambda > 515$  nm irradiation, whereas the use of lower wavelengths led to an increase of all chromium fluoride bands. In the corresponding experiments with argon as the matrix host, the bands of  $\text{CrF}_2$ ,<sup>41</sup>  $\text{CrF}_3$ ,<sup>42</sup> and  $\text{CrF}_4$ <sup>11</sup> could be observed directly after deposition. Upon annealing to 25 K, the band of  $\text{CrF}_4$  grew, while that of  $\text{CrF}_2$  decreased, and broadband irradiation led to an increase of all chromium fluoride bands; see Figure S1 in the Supporting Information.

Different fluorine concentrations ranging from 0.25% to 20%  $\text{F}_2$  in neon were tested in the experiments. As expected, the intensities of the  $\text{CrF}_4$  band increased with increasing  $\text{F}_2$  content of the matrix (Figure S3). The general features of the spectra did not change until a  $\text{F}_2$  concentration of 5% in neon was used when a new broad absorption at 755  $\text{cm}^{-1}$  (labeled A in Figure S4) appeared in the spectra as a shoulder of the  $\text{CrF}_3$  band. This new band grew upon annealing at the expense of the  $\text{CrF}_3$  and  $\text{CrF}_4$  absorptions and can therefore be expected to correspond to a higher chromium fluoride. Upon broadband UV irradiation, the new band disappeared, whereas a broad new band (labeled B in Figure S4) grew at 785  $\text{cm}^{-1}$ . Already at this fluorine concentration the quality of the matrixes was significantly reduced, and at even higher fluorine concentrations no useful information could be retrieved from

the spectra, which consisted only of broad and unresolved bands.

Beyond this, neat elemental fluorine was also used as a reactive matrix host because the formation and stabilization of high-valent chromium fluorides are expected to be favored under such conditions. In contrast to the above-described observations, the use of pure  $F_2$  as the matrix material led again to spectra that were better resolved than those obtained using high fluorine concentrations in noble gases. In such neat fluorine matrixes at 10 K two main groups of absorptions could be identified as being metal-dependent, while all other bands could also be observed when neat  $F_2$  was deposited without chromium. The first group of absorptions consists of two bands at 784.2 and 788.7  $cm^{-1}$ , which were, by comparison with the spectra of the argon matrixes and those published for nitrogen matrixes,<sup>11</sup> assigned to the  $^{52}CrF_4$  molecule. Note, the matrix shifts observed in fluorine and argon matrixes were found to be similar in general, and the splitting of the band might be induced by the diatomic matrix host as in the case of  $N_2$ . The second new absorption was a rather narrow band observed at 764.2  $cm^{-1}$  with an isotopic counterpart at 761.1  $cm^{-1}$  (labeled A in Figure 4). After annealing of the matrix to 25 K, this band

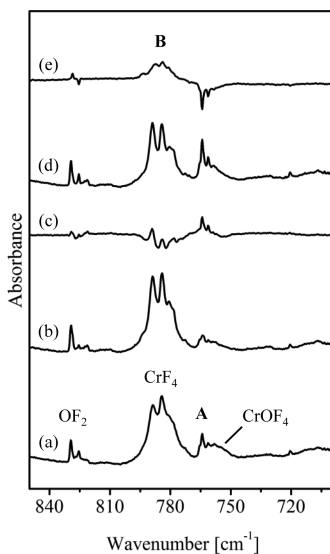


**Figure 4.** IR spectra in the 850–700  $cm^{-1}$  region obtained after co-deposition of laser-ablated chromium atoms with neat  $F_2$ . (a) After 50 min of sample deposition at 10.0 K. (b) After annealing to 25 K. (c) Difference spectrum (spectrum after annealing minus spectrum after deposition). (d) After irradiation with  $\lambda > 400$  nm. (e) Difference spectrum (spectrum after irradiation minus spectrum after annealing).

grew at the expense of the  $CrF_4$  bands. In the irradiation experiments with UV light of  $\lambda > 200$  nm the 764.2  $cm^{-1}$  band vanished and a broad absorption at 780–790  $cm^{-1}$  appeared in the spectrum (labeled B in Figure 4). The behavior of the new group A absorptions in the experiments with either 5%  $F_2$  in neon or neat  $F_2$  as the matrix material is similar, and both bands should correspond to the same higher chromium fluoride species. The position of the band in fluorine matrixes agrees very well with the 763.1  $cm^{-1}$  previously observed in argon matrixes, attributed to both  $CrF_5$  and  $CrF_6$ . Furthermore, the behavior in the irradiation experiments is the same as that published for the 767.7  $cm^{-1}$  band in neon,<sup>14</sup> and it is therefore highly probable that the 764.2  $cm^{-1}$  measured in  $F_2$  matrixes is also caused by the same molecule, which, for several reasons,

we assume to be chromium pentafluoride. One argument is that the calculated thermochemical properties of the high-valent chromium fluorides suggest  $CrF_5$  to be an intermediate species on the way to  $CrF_6$  if the latter can be formed and stabilized at all. The absence of any other bands that can be attributed to a higher chromium fluoride thus indicates the group A absorptions to be due to  $CrF_5$ . Further support for our assignment of the controversial band can be found in the matrix IR spectra obtained after evaporation of presynthesized  $CrF_5$ , which will be presented below.

**Matrix Isolation of Presynthesized High-Valent Fluorides.** Bulk chromium pentafluoride was evaporated to generate matrix samples of  $CrF_5$ , for which the fluorination vessel was directly connected to the spray-on line system of the matrix chamber. When  $CrF_5$  was co-deposited with neon as the matrix host, the absorptions of both  $CrF_4$  and  $CrF_5$  could be observed in the spectra (Figure 5) with a well-resolved isotopic splitting. The positions of the bands agree very well with the bands described before, and the previously reported site splitting for the  $^{52}CrF_4$  was also observed.<sup>14</sup> Based on published values in  $N_2$  matrixes, further bands could be assigned to the  $CrO_2F_2$  (726.3 and 788.6  $cm^{-1}$ ) and  $CrOF_4$  (750.4 and 754.9  $cm^{-1}$ ) molecules, resulting from partial hydrolysis of  $CrF_5$  caused by traces of water. In agreement with previous studies, irradiation of the matrix with visible light of  $\lambda > 400$  nm led to a decrease of the  $CrF_5$  band, while three new bands appeared at 779.0, 788.3, and 790.3  $cm^{-1}$ . When the  $CrF_5$  concentration in the matrix samples was higher, additional bands could be observed in the spectra (Figures S5 and S6). First, the absorptions of  $CrF_4$  were superposed by a second broad band centered at 791.5  $cm^{-1}$ , which, in the annealing and irradiation experiments, showed the same behavior as the 767.7  $cm^{-1}$  band assigned to  $CrF_5$  and is therefore most probably caused by the same molecule. This observation is in line with those made by Willner, who also observed this second band, which supports the assignment of the 767.7  $cm^{-1}$  band to  $CrF_5$ , as  $CrF_6$  should not have any other IR-active mode in this spectral region.<sup>14</sup> Second, five further bands were observed at 415.8, 672.9, 735.5, 766.8, and 816.3  $cm^{-1}$ , which grew upon annealing of the matrixes while the two bands of  $CrF_5$  decreased. Unfortunately, the neon matrixes can be annealed only to 9.0 K, and this behavior can therefore much better be observed in the experiments with argon (vide infra). We assign these bands to the chromium pentafluoride dimer, corroborating a previous tentative assignment of two of these bands to  $Cr_2F_{10}$  or a higher oligomer of  $CrF_5$ .<sup>14</sup> This interpretation of the bands is further supported by our quantum-chemical calculations at the B3LYP/aVTZ level, which predict five vibrational modes with considerable IR intensity in this region of the spectrum, and the calculated wavenumbers fit well to the experimental data; due to its very low intensity, a sixth mode predicted at 428.5  $cm^{-1}$  could not be observed. The observation of the conversion of monomeric  $CrF_5$  to its dimer upon annealing of the matrixes, which is calculated to be exothermic by 8.6  $kJ mol^{-1}$  at the DFT level (vide supra), gives another hint that the 767.7  $cm^{-1}$  band is caused by chromium pentafluoride. Irradiation experiments were done as well, and  $Cr_2F_{10}$  is unstable against  $\lambda > 400$  nm irradiation. The corresponding  $Cr_2F_{10}$  bands disappeared, while the same absorptions as in the photolysis of the monomer grew.

All experiments have also been performed with argon as the matrix host, which allowed higher annealing temperatures and therefore a better observation of the dimerization process of



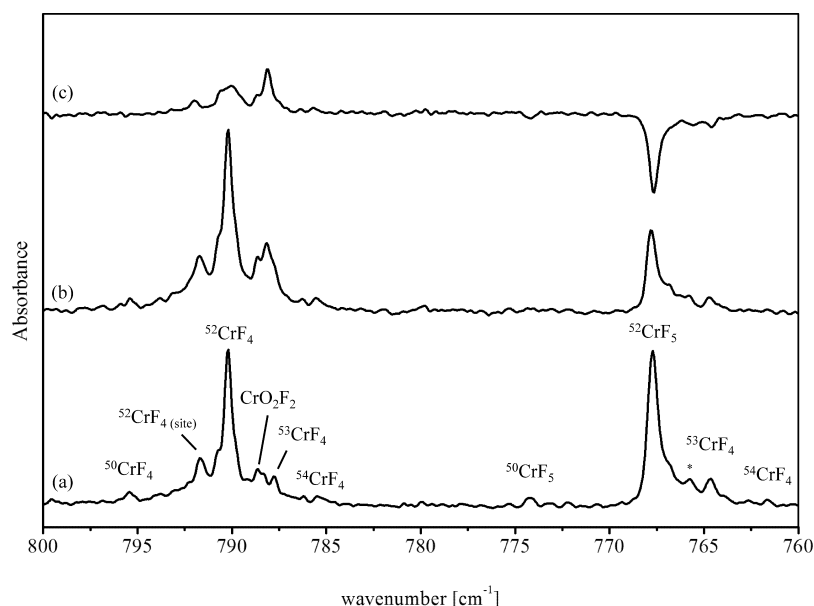


**Figure 5.** Matrix IR spectra in the 800–760  $\text{cm}^{-1}$  region obtained after co-deposition of presynthesized  $\text{CrF}_5$  with neon. (a) After 30 min of sample deposition at 5.0 K. (b) After irradiation with  $\lambda > 400$  nm. (c) Difference spectrum (spectrum after irradiation minus spectrum directly after deposition). \* denotes impurities.

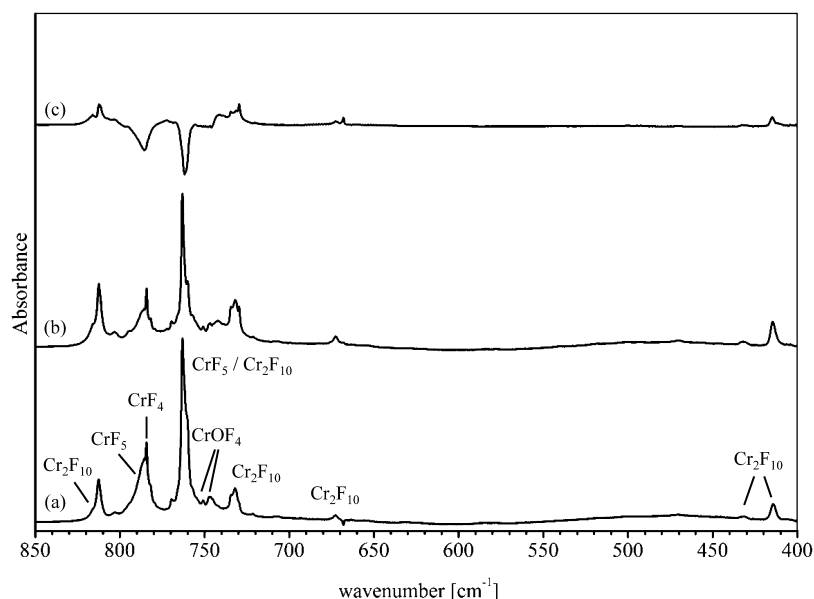


**Figure 6.** Matrix IR spectra in the 850–400  $\text{cm}^{-1}$  region obtained after co-deposition of presynthesized  $\text{CrF}_5$  with argon. (a) After 30 min of sample deposition at 10.0 K. (b) After annealing to 25 K. (c) Difference spectrum (spectrum after annealing minus spectrum directly after deposition).

$\text{CrF}_5$ . Figure 6 shows a spectrum containing the bands of  $\text{CrF}_4$ ,  $\text{CrF}_5$ , and  $\text{Cr}_2\text{F}_{10}$ , in which the second broad band of  $\text{CrF}_5$  at  $785.9 \text{ cm}^{-1}$  can be seen very clearly. Upon annealing, both bands of  $\text{CrF}_5$  decreased, while the five absorptions of  $\text{Cr}_2\text{F}_{10}$  at  $414.3$ ,  $672.8$ ,  $731.9$ ,  $763.1$ , and  $812.6 \text{ cm}^{-1}$  grew. Due to the higher concentrations, even the sixth very weak band of the dimer could be observed at  $431.6 \text{ cm}^{-1}$ . However, one of the bands of the dimer almost coincides with the narrow absorption of  $\text{CrF}_5$ , and the two bands could not be clearly resolved. When the argon matrixes were irradiated with  $\lambda > 400$  nm, the bands of  $\text{CrF}_5$  and  $\text{Cr}_2\text{F}_{10}$  decreased, and in analogy to the experiments with neon, three new bands were observed at  $778.3$ ,  $786.9$ , and  $788.2 \text{ cm}^{-1}$ . Interestingly, the higher possible annealing temperatures in the case of argon matrixes allowed

the further observation that the bands of  $\text{CrF}_5$  could be regenerated when the previously photolyzed matrix samples were annealed to 25 K for 5 min (Figure S7). We therefore assume these new bands to be caused either by  $\text{CrF}_5$  in an excited electronic state or by a  $\text{CrF}_4 \cdot \text{F}$  complex formed after homolytic breaking of one of the bonds of  $\text{CrF}_5$  after which the dissociated fluorine atom remains trapped at the same matrix cage. The regeneration of the former chromium pentafluoride occurs upon thermal stimulation. Beyond this, it was found that keeping the matrix at 5.0 K for 11 h also led to the regeneration of a small fraction of  $\text{CrF}_5$ . The same behavior could also be observed in the laser-ablation experiments with neat  $\text{F}_2$ , where the  $764.2 \text{ cm}^{-1}$  band attributed to  $\text{CrF}_5$  reappeared after annealing of previously photolyzed matrix samples. Preliminary



quantum-chemical calculations were done in order to identify the nature of this new band of "CrF<sub>5</sub>" but unfortunately without any success, and a more detailed investigation is beyond the scope of the present investigation.

## CONCLUSION

The present investigation aims at the clarification of the long-standing discussion of whether chromium hexafluoride exists or not. Two debatable absorptions at 767.7 and 763.2 cm<sup>-1</sup> have been found in previous matrix-isolation experiments at cryogenic conditions, which have been assigned to CrF<sub>5</sub> and CrF<sub>6</sub>. Here we show by matrix-isolation experiments in conjunction with state-of-the-art quantum-chemical calculations that the previous assignment of CrF<sub>5</sub> was correct.

Evidence for this assignment is given by the observation of a second broad band, which must be assigned to the same species. The flat potential energy surface for the Jahn–Teller distortion of CrF<sub>5</sub> might be held responsible for the broadness of this second band and the nonobservation of the third Cr–F stretching mode of the predicted high IR intensity. Furthermore, the bands of the Cr<sub>2</sub>F<sub>10</sub> dimer could be unambiguously assigned in both neon and argon matrixes and whose formation upon annealing of the matrix samples is accompanied by a decrease of both bands assigned to chromium pentafluoride. By contrast, the bands of CrF<sub>5</sub> were not observed in the matrix spectra obtained after the reaction of laser-ablated chromium atoms with fluorine diluted in neon and argon as the matrix hosts, where the highest formed chromium fluoride was CrF<sub>4</sub>. When fluorine was used as the matrix host, the narrow band of CrF<sub>5</sub> with the typical isotopic splitting of chromium could be observed at 764.3 cm<sup>-1</sup>, showing that neat F<sub>2</sub> matrixes are indeed able to stabilize high oxidation states that cannot be reached at lower fluorine concentrations. The absence of any other band that could be assigned to a higher chromium fluoride indicates this band to be due to CrF<sub>5</sub>. Upon UV irradiation, an excited form of CrF<sub>5</sub> is generated, either CrF<sub>5</sub> in an excited electronic state or a CrF<sub>4</sub>·F complex, which relaxes to the ground state or recombines to CrF<sub>5</sub> upon annealing of the matrixes. No evidence was found in the experiments for chromium hexafluoride. According to our CCSD(T) calculations, CrF<sub>6</sub> is a thermochemically unstable species. Nevertheless, its formation at high fluorine pressures and elevated temperatures in autoclave reactions cannot be excluded with certainty.

## ASSOCIATED CONTENT

### Supporting Information

This material is available free of charge via the Internet at <http://pubs.acs.org>.

## AUTHOR INFORMATION

### Corresponding Author

\*E-mail: [s.riedel@fu-berlin.de](mailto:s.riedel@fu-berlin.de).

### Notes

The authors declare no competing financial interest.

## ACKNOWLEDGMENTS

We gratefully acknowledge financial support from the DFG. We further thank Dr. Florian Kraus for providing the CrF<sub>3</sub> samples used in the bulk synthesis of chromium pentafluoride and Prof. Helge Willner for fruitful discussions. The authors are also

grateful to the BWGrid and Prof. I. Krossing for providing computational resources.

## REFERENCES

- (1) Glemser, O.; Roesky, H.; Hellberg, K. H. *Angew. Chem.* **1963**, *75*, 346–347.
- (2) Riedel, S.; Kaupp, M. *Coord. Chem. Rev.* **2009**, *253*, 606–624.
- (3) Edwards, A. J.; Falconer, W. E.; Sunder, W. A. *J. Chem. Soc., Dalton Trans.* **1974**, 541–542.
- (4) Edwards, A. J. *Proc. Chem. Soc., London* **1963**, 205.
- (5) Christie, K. O.; Wilson, W. W.; Bougon, R. A. *Inorg. Chem.* **1986**, *25*, 2163–2169.
- (6) Garner, C. D.; Mather, R.; Dove, M. F. A. *J. Chem. Soc., Chem. Commun.* **1973**, 633–634.
- (7) Huang, J.; Hedberg, K.; Shreeve, J. n. M.; Mallela, S. P. *Inorg. Chem.* **1988**, *27*, 4633–4635.
- (8) Shorafa, H.; Seppelt, K. Z. *Anorg. Allg. Chem.* **2009**, *635*, 112–114.
- (9) Falconer, W. E.; Jones, G. R.; Sunder, W. A.; Vasile, M. J.; Muentner, A. A.; Dyke, T. R.; Klemperer, W. J. *Fluorine Chem.* **1974**, *4*, 213–234.
- (10) Hope, E. G.; Jones, P. J.; Levason, W.; Ogden, J. S.; Tajik, M. J. *Chem. Soc., Chem. Commun.* **1984**, 1355–1356.
- (11) Hope, E. G.; Jones, P. J.; Levason, W.; Ogden, J. S.; Tajik, M.; Turff, J. W. *J. Chem. Soc., Dalton Trans.* **1985**, 1443–1449.
- (12) Hope, E. G.; Levason, W.; Ogden, J. S. *Inorg. Chem.* **1991**, *30*, 4873–4874.
- (13) Jacob, E.; Willner, H. *Chem. Ber.* **1990**, *123*, 1319–1321.
- (14) Jacobs, J.; Mueller, H. S. P.; Willner, H.; Jacob, E.; Buerger, H. *Inorg. Chem.* **1992**, *31*, 5357–5363.
- (15) Marsden, C. J.; Wolynec, P. P. *Inorg. Chem.* **1991**, *30*, 1681–1682.
- (16) Marsden, C. J.; Moncrieff, D.; Quelch, G. E. J. *Phys. Chem.* **1994**, *98*, 2038–2043.
- (17) Pierloot, K.; Roos, B. O. *Inorg. Chem.* **1992**, *31*, 5353–5354.
- (18) Neuhaus, A.; Frenking, G.; Huber, C.; Gauss, J. *Inorg. Chem.* **1992**, *31*, 5355–5356.
- (19) Vanquickenborne, L. G.; Vinckier, A. E.; Pierloot, K. *Inorg. Chem.* **1996**, *35*, 1305–1309.
- (20) Siddiqui, S. A. *Struct. Chem.* **2012**, *23*, 267–274.
- (21) Schlöder, T.; Riedel, S. Extreme Oxidation States of Transition Metals. In *Comprehensive Inorganic Chemistry II* (2d ed.), Reedijk, J.; Poeppelemeier, K., Eds.; Elsevier: Amsterdam, 2013; Vol. 9, pp 227–243.
- (22) Schlöder, T. *Matrix Isolation and Quantum-Chemical Study of Molecules Containing Transition Metals in High Oxidation States*; Albert-Ludwigs-Universität Freiburg: Freiburg, 2013.
- (23) Bougon, R.; Wilson, W. W.; Christie, K. O. *Inorg. Chem.* **1985**, *24*, 2286–2292.
- (24) Frisch, M. J.; Trucks, G. W.; Schlegel, H. B.; Scuseria, G. E.; Robb, M. A.; Cheeseman, J. R.; Scalmani, G.; Barone, V.; Mennucci, B.; Petersson, G. A.; Nakatsuji, H.; Caricato, M.; Li, X.; Hratchian, H. P.; Izmaylov, A. F.; Bloino, J.; Zheng, G.; Sonnenberg, J. L.; Hada, M.; Ehara, M.; Toyota, K.; Fukuda, R.; Hasegawa, J.; Ishida, M.; Nakajima, T.; Honda, Y.; Kitao, O.; Nakai, H.; Vreven, T.; Montgomery, J. J. A.; Peralta, J. E.; Ogliaro, F.; Bearpark, M.; Heyd, J. J.; Brothers, E.; Kudin, K. N.; Staroverov, V. N.; Kobayashi, R.; Normand, J.; Raghavachari, K.; Rendell, A.; Burant, J. C.; Iyengar, S. S.; Tomasi, J.; Cossi, M.; Rega, N.; Millam, J. M.; Klene, M.; Knox, J. E.; Cross, J. B.; Bakken, V.; Adamo, C.; Jaramillo, J.; Gomperts, R.; Stratmann, R. E.; Yazyev, O.; Austin, A. J.; Cammi, R.; Pomelli, C.; Ochterski, J. W.; Martin, R. L.; Morokuma, K.; Zakrzewski, V. G.; Voth, G. A.; Salvador, P.; Dannenberg, J. J.; Dapprich, S.; Daniels, A. D.; Farkas, Ö.; Foresman, J. B.; Ortiz, J. V.; Cioslowski, J.; Fox, D. J., *Gaussian09*, Revision B.1; Gaussian Inc.: Wallingford, CT, 2009.
- (25) Becke, A. J. *Chem. Phys.* **1993**, *98*, 5648.
- (26) Becke, A. D. *Phys. Rev. A* **1988**, *38*, 3098–3100.
- (27) Lee, C.; Yang, W.; Parr, R. G. *Phys. Rev. B* **1988**, *37*, 785–789.

- (28) Schlöder, T.; Vent-Schmidt, T.; Riedel, S. *Angew. Chem., Int. Ed.* **2012**, *51*, 12063–12067.
- (29) Riedel, S.; Straka, M.; Kaupp, M. *Phys. Chem. Chem. Phys.* **2004**, *6*, 1122–1127.
- (30) Kendall, R. J. *Chem. Phys.* **1992**, *96*, 6796.
- (31) Balabanov, N. B.; Peterson, K. A. *J. Chem. Phys.* **2005**, *123*, 064107–064115.
- (32) Helgaker, T.; Klopper, W.; Koch, H.; Noga, J. *J. Chem. Phys.* **1997**, *106*, 9639–9646.
- (33) Woon, D. E.; Dunning, J. T. H. *J. Chem. Phys.* **1995**, *103*, 4572–4585.
- (34) Stanton, J. F.; Gauss, J.; Harding, M. E.; Szalay, P. G. *CFOUR*, a quantum chemical program package; with contributions from Auer, A. A.; Bartlett, R. J.; Benedikt, U.; Berger, C.; Bernholdt, D. E.; Bomble, Y. J.; Cheng, L.; Christiansen, O.; Heckert, M.; Heun, O.; Huber, C.; Jagau, T.-C.; Jonsson, D.; Jusélius, J.; Klein, K.; Lauderdale, W. J.; Matthews, D. A.; Metzroth, T.; Mück, L. A.; O'Neill, D. P.; Price, D. R.; Prochnow, E.; Puzzarini, C.; Ruud, K.; Schiffmann, F.; Schwalbach, W.; Stopkowitz, S.; Tajti, A.; Vázquez, J.; Wang, F.; Watts, J. D.; and the integral packages MOLECULE (Almlöf, J.; Taylor, P. R.), PROPS (Taylor, P. R.), ABACUS (Helgaker, T.; Aa, H. J.; Jensen, P.; Jørgensen; Olsen, J.), and ECP routines by Mitin, A. V.; van Wüllen, C. For the current version, see <http://www.cfour.de>.
- (35) Nielsen, I. M. B.; Allendorf, M. D. *J. Phys. Chem. A* **2005**, *109*, 928–933.
- (36) Vest, B.; Schwerdtfeger, P.; Kolonits, M.; Hargittai, M. *Chem. Phys. Lett.* **2009**, *468*, 143–147.
- (37) Jacob, E. J.; Hedberg, L.; Hedberg, K.; Davis, H.; Gard, G. L. *J. Phys. Chem.* **1984**, *88*, 1935–1936.
- (38) Hedberg, L.; Hedberg, K.; Gard, G. L.; Udeaja, J. O. *Acta Chem. Scand., Ser. A* **1988**, *A42*, 318–323.
- (39) Zasorin, E. Z.; Ivanov, A. A.; Ermolaeva, L. I.; Spiridonov, V. P. *Zh. Fiz. Khim.* **1989**, *63*, 669–673.
- (40) Solomonik, V. G.; Stanton, J. F.; Boggs, J. E. *J. Chem. Phys.* **2005**, *122*, 094322–094412.
- (41) Hastie, J. W.; Hauge, R.; Margrave, J. L. *J. Chem. Soc., Chem. Commun.* **1969**, 1452–1453.
- (42) Bukhmarina, V. N.; Gerasimov, A. Y.; Predtechenskii, Y. B.; Shklyarik, V. G. *Opt. Spektrosk.* **1988**, *65*, 876–881.
- (43) Osin, S. B.; Davliasthin, D. I.; Ogden, J. S. *J. Fluorine Chem.* **1996**, *76*, 187–192.